NeuroImage: Clinical 12 (2016) 965–969

Contents lists available at ScienceDirect

NeuroImage: Clinical

journal homepage: www.elsevier.com/locate/ynicl

Magnetic susceptibility in the deep layers of the primary motor cortex in Amyotrophic Lateral Sclerosis

M. Costagli[a,b], G. Donatelli[c,*], L. Biagi[b], E. Caldarazzo Ienco[d], G. Siciliano[d], M. Tosetti[a,b], M. Cosottini[a,c]

[a] Imago7 Research Foundation, Pisa, Italy
[b] Laboratory of Medical Physics and Biotechnologies for Magnetic Resonance, IRCCS Stella Maris, Pisa, Italy
[c] Department of Translational Research and New Technologies in Medicine and Surgery, University of Pisa, Pisa, Italy
[d] Neurology Unit, Department of Clinical and Experimental Medicine, University of Pisa, Pisa, Italy

ARTICLE INFO

Article history:
Received 20 January 2016
Received in revised form 29 March 2016
Accepted 30 April 2016
Available online 2 May 2016

ABSTRACT

Amyotrophic Lateral Sclerosis (ALS) is a progressive neurological disorder that entails degeneration of both upper and lower motor neurons. The primary motor cortex (M1) in patients with upper motor neuron (UMN) impairment is pronouncedly hypointense in Magnetic Resonance (MR) T2* contrast. In the present study, 3D gradient-recalled multi-echo sequences were used on a 7 Tesla MR system to acquire T2*-weighted images targeting M1 at high spatial resolution. MR raw data were used for Quantitative Susceptibility Mapping (QSM). Measures of magnetic susceptibility correlated with the expected concentration of non-heme iron in different regions of the cerebral cortex in healthy subjects. In ALS patients, significant increases in magnetic susceptibility co-localized with the T2* hypointensity observed in the middle and deep layers of M1. The magnetic susceptibility, hence iron concentration, of the deep cortical layers of patients' M1 subregions corresponding to Penfield's areas of the hand and foot in both hemispheres significantly correlated with the clinical scores of UMN impairment of the corresponding limbs. QSM therefore reflects the presence of iron deposits related to neuroinflammatory reaction and cortical microgliosis, and might prove useful in estimating M1 iron concentration, as a possible radiological sign of severe UMN burden in ALS patients.

1. Introduction

Amyotrophic Lateral Sclerosis (ALS) is a progressive motor neuron disorder that entails degeneration of both upper and lower motor neurons (Strong and Rosenfeld, 2015), producing fasciculation, muscle wasting and weakness, increased spasticity and hyperreflexia. The hallmark of upper motor neuron (UMN) involvement in ALS is the depopulation of Betz cells in the primary motor cortex (M1) and axonal loss in the descending motor pathway, associated with myelin pallor and gliosis of the corticospinal tract (Ince et al., 2003). As a consequence of neuroinflammatory reaction (Philips and Robberecht, 2011), UMN damage is associated with cortical microgliosis (Turner et al., 2004), which leads to iron deposits in activated microglia in the middle and deep layers of the motor cortex (Kwan et al., 2012). Gradient Recalled Echo (GRE) techniques in Magnetic Resonance Imaging (MRI) enable the fine depiction of the most prominent structural changes that involve the cortex and the presence of iron (Adachi et al., 2015; Duyn et al., 2007; Haacke et al., 2009; Ignjatović et al., 2013). M1, which has been described to usually appear slightly more hypointense than neighboring cortices (postcentral gyrus) in the healthy brain in T2* contrast (Kwan et al., 2012; Schweitzer et al., 2015), is pronouncedly hypointense in patients with upper motor neuron impairment (Ignjatović et al., 2013; Schweitzer et al., 2015). In particular, studies that investigated M1 at high spatial resolution with ultra-high field MRI revealed *ex vivo* (Kwan et al., 2012) and *in vivo* (Cosottini et al., 2016) that M1 hypointensity in T2* is spatially confined to the deep layers of M1. T2* signal loss originates from changes in magnetic susceptibility (χ) of tissues: diamagnetic tissues, such as calcium and lipids, have negative χ, while paramagnetic tissues, such as iron, have positive χ.

Quantitative Susceptibility Mapping (QSM) is a technique that allows the quantification of χ *in vivo*, by using the phase of the MRI signal (Haacke et al., 2015; Liu et al., 2015). There are several competing factors that influence MRI-measured χ, such as the local concentrations of iron, lipids, calcium, tissue microstructure and spatial orientation (Deistung et al., 2013b; Schweser et al., 2010; Wharton and Bowtell, 2015). In particular, it has been demonstrated that χ correlates with iron concentration in gray matter of deep nuclei and cerebral cortex (Barbosa et al., 2015). Therefore we aimed to use 3D-GRE acquisitions at 7 T for QSM at high spatial resolution to demonstrate, *in vivo*, that the T2* hypointensity in ALS corresponds to an increase in iron concentration, as it was recently shown in one post-mortem specimen from the

* Corresponding author at: Department of Translational Research and New Technologies in Medicine and Surgery, Via Savi 10, 56126 Pisa, Italy.
E-mail address: graziella_donatelli@hotmail.com (G. Donatelli).

http://dx.doi.org/10.1016/j.nicl.2016.04.011

M1 of an ALS patient (Kwan et al., 2012), and to assess whether χ correlates with clinical scores of motor neuron impairment.

2. Materials and methods

2.1. Subjects

17 ALS patients (mean age ± standard deviation = 62 ± 11 years) and 13 healthy controls (HC; 55 ± 11 years) participated to this study, with their understanding and written consent in accordance with the protocol approved by the Ethics Committee of Tuscany, section of Pisa, Italy, and in compliance with national legislation and the Declaration of Helsinki. All patients had a diagnosis of definite ALS (limb onset) according to the revised El Escorial diagnostic criteria (Brooks et al., 2000). Their ALS Functional Rating Scale Revised (ALSFRS-R) (Cedarbaum et al., 1999) was 40 ± 5 (mean ± standard deviation) and ranged between 23 and 46. Their disease duration was 17 ± 12 months and ranged between 5 and 46. The UMN impairment was evaluated and recorded for each individual limb of each ALS patient by using a composite semiquantitative score (UMN-score) ranging from 0 to 8 (Cosottini et al., 2016). Exclusion criteria for patient selection were the diagnosis of other neurological and psychiatric comorbidities. All HC had no history of neurological and psychiatric disorders.

2.2. MRI data acquisition

Data were collected with a 7T MR950 system (GE Healthcare Medical Systems, Milwaukee, WI, USA) equipped with a 2ch-tx/32ch-rx head coil (Nova Medical, Wilmington, MA USA). The protocol included a 3D multi-echo GRE sequence covering the cerebrum from the vertex to the internal capsule, with Time of Repetition (TR) = 54.1 ms, Times of Echo (TE) = 5.6 ms, 12 ms, 18.3 ms, 24.7 ms, 31.1 ms, 37.5 ms, 43.9 ms, Flip Angle (FA) = 15 deg, parallel imaging ASSET acceleration = 2, spatial resolution of $0.5 \times 0.5 \times 1$ mm^3, and scan duration = 6′59″. Both the real and imaginary parts of images obtained at each TE were saved and converted into phase and magnitude data. T2*-weighted images were obtained by averaging the magnitude data from each individual echo.

The protocol also included a 2D two-echo GRE sequence prescribed axially and targeting M1, with TE = 10 ms and 20 ms, TR = 500 ms, FA = 15 deg, number of excitations (NEX) = 2, in-plane spatial resolution of 0.25×0.25 mm^2, slice thickness = 2 mm, and scan duration = 7′32″.

2.3. Qualitative image evaluation

Two neuroradiologists (25 and 6 years of experience, Mi.C. and G.D., respectively), blinded to the clinical status of subjects, evaluated the T2*-weighted images obtained from both 3D multi-echo GRE acquisitions and 2D GRE sequences.

T2*-weighted images of M1 obtained from 3D multi-echo GRE acquisitions were qualitatively evaluated using scores ranging between 0 and 2, similarly to what has been done in the recent literature (Schweitzer et al., 2015): a score of 0 was assigned when M1 did not differ from the neighboring cortices, a score of 1 was assigned when M1 appeared slightly more hypointense than neighboring cortices, and a score of 2 was assigned when M1 appeared much more hypointense than the neighboring cortices.

The 2D GRE images of all subjects were qualitatively evaluated as recently reported (Cosottini et al., 2016): patients were separated into two groups, the former with normal appearance of M1 (group A) and the latter with particularly thin and hypointense deeper layers of M1 (group B).

2.4. Definition of ROIs

In each hemisphere of both ALS patients and HC, two oval ROIs were manually drawn in 3D T2*-weighted images to delineate the deep cortical layers of M1 corresponding to Penfield's areas of the hand (hM1, in the "hand knob") (Yousry et al., 1997) and foot (fM1, in the paracentral lobule) (Penfield and Rasmussen, 1950). ROIs were drawn by the two neuroradiologists in consensus of opinion on the slice that best represented the target region, and their size was approximately 5 mm^2. One additional ROI of 15 mm^2 delineated the splenium of the corpus callosum (SCC). Examples of these ROIs are shown in Supplementary Fig. 1.

Moreover, in the right hemisphere of HC only, the following 4 ROIs were also drawn, covering the full-thickness cortex of: *i*) M1 (hand knob); *ii*) primary somatosensory cortex (S1, posterior to the hand knob); *iii*) cortex in the superior parietal lobule; *iv*) prefrontal cortex in the anterior cingulate gyrus. Their size was approximately 10 mm^2. Examples of these ROIs are shown in Supplementary Fig. 2.

2.5. QSM

Phase data of 3D multi-echo GRE acquisitions were first preprocessed for Laplacian-based phase unwrapping (Li et al., 2011; Schofield and Zhu, 2003) and V-SHARP background phase removal (Schweser et al., 2011; Wu et al., 2012). χ maps were computed for each echo with the iLSQR method (Li et al., 2011), and one final resultant χ map was generated by averaging the χ maps obtained from each individual echo (Denk and Rauscher, 2010).

The ROIs of each subject, drawn as described in the previous subsection, were copied onto the respective χ maps. The measured values of χ in all ROIs were expressed in parts per billion [ppb] with respect to the average χ in the SCC, in every single subject.

2.6. Estimated non-heme iron concentration in the cortex of HC

In HC, the predicted content of iron (ρ, expressed in mg of iron per 100 g of tissue) as a function of age (Y, in years) was calculated in M1, S1, non-S1 parietal cortex and prefrontal cortex, according to the histological ferritin concentrations found by Hallgren and Sourander (1958):

$$\rho_{M1} = 4.79 \times \{1 - \exp(-0.05 \times Y)\} + 0.40; \quad (1)$$

$$\rho_{S1} = 3.97 \times \{1 - \exp(-0.07 \times Y)\} + 0.49; \quad (2)$$

$$\rho_{parietal} = 3.31 \times \{1 - \exp(-0.06 \times Y)\} + 0.60; \quad (3)$$

$$\rho_{prefrontal} = 2.43 \times \{1 - \exp(-0.07 \times Y)\} + 0.58. \quad (4)$$

2.7. Statistical analysis

The correlation between measured χ and predicted content of iron in the four cortical regions in HC was evaluated with Spearman rank test. Wilcoxon tests were used to compare χ in the M1 subregion corresponding to the clinically most affected limb of ALS patients (on the basis of their UMN-score) with χ in HC. A Mann-Whitney test was used to compare χ in the two groups of patients (group A *vs* group B). Correlations between χ in all M1 subregions of ALS patients and UMN-scores of the corresponding limbs were measured by Spearman rank test.

Significance level in all statistical tests was set to 5%.

3. Results

3.1. Qualitative analysis

T2* images acquired with 3D multi-echo GRE are shown in Fig. 1a–b. In ALS patients, the deep layers of M1 (indicated by arrows in Fig. 1b) appeared strikingly more hypointense than ipsilateral S1 (hypointensity score = 2 in 41.2% of patients; score = 1 in 32.3% patients; score = 0 in 26.5% of patients), but this feature was also present,

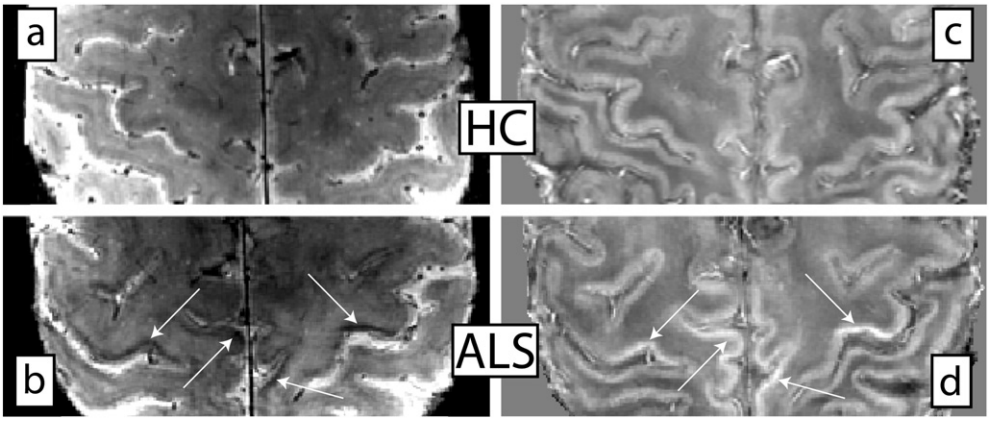

Fig. 1. Appearance of M1 in one healthy control and one ALS patient. T2*-weighted images targeting the M1 of one healthy control subject and one ALS patient are shown in (a) and (b), respectively. The corresponding susceptibility maps are shown in (c) and (d), respectively. Arrows indicate the T2* signal hypointensity and QSM hyperintensity in patients' M1 deep layers.

to a lesser extent, in the M1 of HC (hypointensity score = 2 in 7.7% of HC; score = 1 in 42.3% HC; score = 0 in 50% of HC). In the evaluation of 2D GRE images, only 10 out of 17 patients (59%) exhibited particularly thin and hypointense deep layers of M1 (group B). The UMN-score in patients with this radiological feature was 4.6 ± 2.9, while it was 0.4 ± 0.5 in other ALS patients (group A). Maps of χ (Fig. 1c–d) demonstrated that the band of T2* hypointensity in M1 of ALS patients corresponds to paramagnetic tissue (hyperintensity in QSM, indicated by arrows in Fig. 1d).

3.2. Correlation between χ and expected iron concentration in HC

Our measures of χ in the ROIs of four cortical regions (M1, S1, non-S1 parietal cortex and prefrontal cortex) showed a strong and significant positive correlation with the expected cortical content of non-heme iron, estimated by using Eqs. (1)–(4): $r = 0.71$; $p < 0.0001$ (Fig. 2). The linear function that best fitted the relationship between χ and ρ was:

$$\chi = 21.79 \times \rho - 67.22. \quad (5)$$

The goodness of the linear fit was $R^2 = 0.56$.

3.3. Absence of correlation between subjects' age and χ in deep cortical layers

In HC, by considering the four M1 subregions (deep cortical layers in hM1 and fM1, left and right hemisphere), no significant correlation was observed between subjects' age and χ ($r = -0.06$, $p = 0.66$, Supplementary Fig. 3). Therefore no correction for age was applied in subsequent analyses.

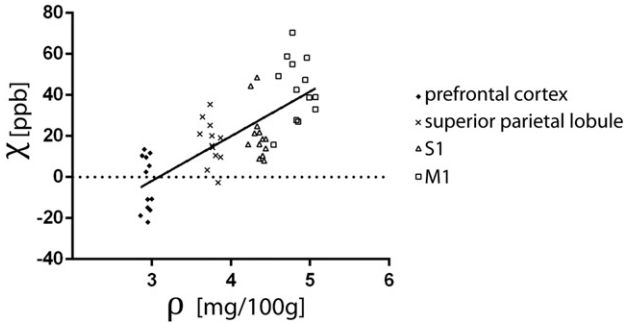

Fig. 2. Magnetic susceptibility (χ) correlates with the expected concentration of iron (ρ) in different cortical regions in healthy controls.

3.4. QSM in ALS patients

ALS patients' χ values in deep cortical layers corresponding to the most affected limbs were significantly higher (13 ppb, $p < 0.018$) than average χ in the corresponding ROIs in HC (Fig. 3). By taking the four M1 subregions together (deep cortical layers in hM1 and fM1, left and right hemisphere), the average χ in HC was 37 ± 16 ppb, while in ALS patients, in the M1 subregions corresponding to their most impaired limb according to the UMN-score, χ was 52 ± 18 ppb.

Among patients, χ in the ROI corresponding to the most affected limb was significantly ($p < 0.033$) higher ($\chi = 61 \pm 16$ ppb) in group B than in patients with normal radiological appearance of M1 (group A, $\chi = 39 \pm 12$ ppb) as shown in Fig. 4. A binary classifier with $\chi_{cutoff} = 47$ ppb (dashed line in Fig. 4) allowed to correctly separate the ALS patients into the two groups A and B with 2 classification errors (arrows in Fig. 4).

χ in the M1 of patients with normal radiological appearance of M1 (group A) did not differ from that in the M1 of HC ($p = 0.69$).

In patients' M1, χ significantly correlated with the UMN-score of the corresponding limb, as shown in Fig. 5: $r = 0.46$; $p < 0.0002$. The linear function that best fitted the relationship between χ and UMN-score was:

$$\text{UMN-score} = 0.05 \times \chi - 0.46. \quad (6)$$

The goodness of the linear fit was $R^2 = 0.20$.

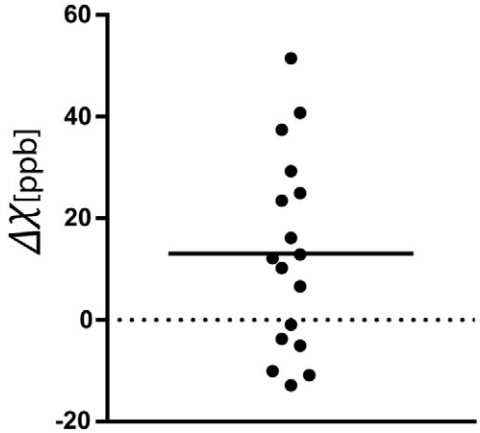

Fig. 3. Difference ($\Delta\chi$) between ALS patients' χ values in deep cortical layers corresponding to the most impaired limb and average χ in the corresponding ROIs in HC. The solid line represents average $\Delta\chi = 13$ ppb.

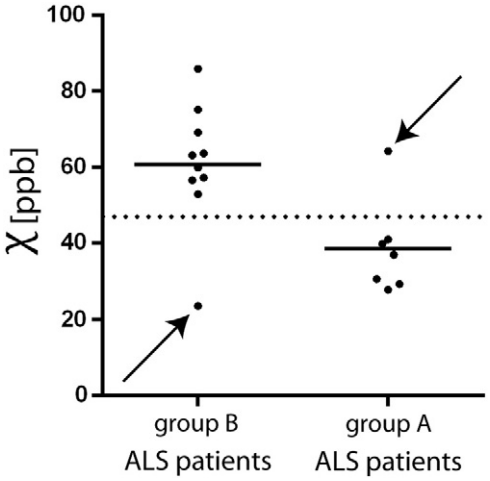

Fig. 4. Among patients, χ in M1 was significantly ($p < 0.033$) higher in patients of group B (with particularly thin and hypointense cortical deep layers) than in patients of group A (with normal radiological appearance of M1). A binary classifier with $\chi_{cutoff} = 47$ ppb (dashed line) allows to separate the ALS patients into the two groups A and B with 2 classification errors (arrows).

4. Discussion

4.1. Methodological considerations

Due to arbitrary phase offsets after filtering operations in data preprocessing, QSM techniques cannot provide absolute measures, but they are able to provide relative measures of χ variations across brain tissues. To compare χ maps across subjects, it is necessary to define one reference region, the same in every subject, and express the values of χ in other brain regions with respect to such reference region (Haacke et al., 2015). While the cerebrospinal fluid (CSF) would be, in principle, an ideal reference due to its negligible iron content (LeVine et al., 1998), a wide range of CSF susceptibilities has been observed depending on the regions of measurement (Deistung et al., 2013a; Haacke et al., 2015; Li et al., 2014; Lim et al., 2013), most likely caused by background field removal and artifacts associated to neighboring structures (Haacke et al., 2015), in particular the choroid plexus. The white matter subjacent to M1 is not a suitable reference, either, because it has been demonstrated that ALS affects the corticospinal tract (CST) (Cosottini et al., 2005; Ince et al., 2003), and the large variability in fiber orientation within the CST induces a large uncertainty in the measure of χ (Denk et al., 2011; Wharton and Bowtell, 2015). Among the regions that are included in our targeted acquisition covering M1, we chose to use the SCC as reference, for two reasons. First, the SCC is involved in the interhemispheric communication among visual areas in the occipital and parietal lobes (Knyazeva, 2013; Putnam et al., 2010), with a negligible involvement of the motor pathway. Second, the angle between B_0 and white matter fibers in SCC is largely independent of subject head position (pitch), as it is always approximately 90°, which reduces the orientation-dependent variability of χ measurements.

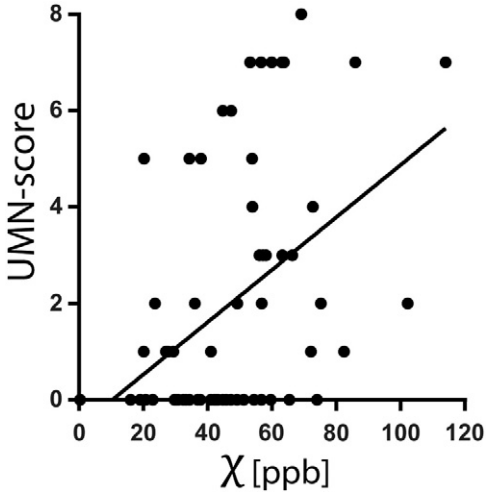

Fig. 5. In patients, χ in the deep layers of M1 subregions correlated ($r = 0.46$; $p < 0.0002$) with the UMN-score.

4.2. Iron accumulation in M1 deep layers and correlation with UMN impairment

The pronounced T2* signal hypointensity in M1 of ALS patients has been reported by recent MRI studies (Ignjatović et al., 2013; Kwan et al., 2012; Schweitzer et al., 2015). However, we observed that M1 appears hypointense also in healthy controls and is not, by itself, an accurate biomarker of ALS. T2* signal loss in MRI could be due to the presence of either diamagnetic compounds ($\chi < 0$, such as calcium and lipids) or paramagnetic compounds ($\chi > 0$, such as iron). Fig. 1 provides the demonstration that T2* signal hypointensity, specific to the deep cortical layers of M1 in ALS patients, corresponds to localized increase in magnetic susceptibility. Based on the linear relation between χ and the expected iron concentration in different cortical regions in HC (Eq. (5) and Fig. 2), our results agree with previous *ex vivo* findings, which demonstrated the iron accumulation in microglial cells infiltrated in the deep layers of M1 (Kwan et al., 2012).

One recent study conducted on a 3 T MRI system observed an increase in χ in the M1 of ALS patients (Schweitzer et al., 2015) however the specificity of such increase to the cortical deep layers and its relation with patients' clinical conditions was not reported. In fact, rather than being a candidate direct biomarker of ALS, our results show that χ in M1 correlates with UMN impairment.

By inverting Eq. (5), it is possible to provide estimates of iron concentration in physiology and pathology: M1 subregions corresponding to the most impaired limb of each patient would have an average iron concentration of 5.5 ± 0.8 mg/100 g, which is significantly higher than the average iron concentration of 4.8 ± 0.6 mg/100 g that was estimated in HC. According to Eq. (5), the magnetic susceptibility $\chi_{cutoff} =$ 47 ppb that allowed the identification of radiological signs of pathology in 2D GRE images would correspond to an estimated concentration of iron of 5.2 mg/100 g, which is 9.4% higher than average iron concentration in HC. In other words, if the abnormal concentration of iron is below such value, it is not possible to appreciate the radiological signs of motor neuron impairment: among the 17 ALS patients who took part to our study, those who did not exhibit T2* signal hypointensity (group A) had minimal UMN impairment (their average UMN-score considering the most severely impaired limb was 0.4) and negligible increase in χ with respect to HC.

5. Conclusion

The main finding of this study is that magnetic susceptibility of the deep cortical layers of patients' M1 subregions corresponding to Penfield's areas of the hand and foot significantly correlates with the UMN impairment of the corresponding limbs. QSM, by reflecting the presence of iron deposits related to neuroinflammatory reaction and cortical microgliosis, might prove useful in estimating M1 iron concentration as a possible radiological sign of severe UMN burden in ALS patients.

Supplementary data to this article can be found online at http://dx.doi.org/10.1016/j.nicl.2016.04.011.

Acknowledgements

This work was part of the protocol "Clinical Impact of Ultra-High Field MRI in Neurodegenerative Diseases Diagnosis" (RF-2009-1546281) approved and funded by the Italian Ministry of Health, and cofunded by the Health Service of Tuscany.

References

Adachi, Y., Sato, N., Saito, Y., Kimura, Y., Nakata, Y., Ito, K., Kamiya, K., Matsuda, H., Tsukamoto, T., Ogawa, M., 2015. Usefulness of SWI for the detection of iron in the motor cortex in amyotrophic lateral sclerosis. J. Neuroimaging 25, 443–451. http://dx.doi.org/10.1111/jon.12127.

Barbosa, J.H.O., Santos, A.C., Tumas, V., Liu, M., Zheng, W., Haacke, E.M., Salmon, C.E.G., 2015. Quantifying brain iron deposition in patients with Parkinson's disease using quantitative susceptibility mapping, R2 and R2*. Magn. Reson. Imaging http://dx.doi.org/10.1016/j.mri.2015.02.021.

Brooks, B.R., Miller, R.G., Swash, M., Munsat, T.L., World Federation of Neurology Research Group on Motor Neuron Diseases, 2000. El Escorial revisited: revised criteria for the diagnosis of amyotrophic lateral sclerosis. Presented at the Amyotrophic Lateral Sclerosis and Other Motor Neuron Disorders: Official Publication of the World Federation of Neurology, Research Group on Motor Neuron Diseases, pp. 293–299.

Cedarbaum, J.M., Stambler, N., Malta, E., Fuller, C., Hilt, D., Thurmond, B., Nakanishi, A., 1999. The ALSFRS-R: a revised ALS functional rating scale that incorporates assessments of respiratory function. BDNF ALS Study Group (Phase III). J. Neurol. Sci. 169, 13–21.

Cosottini, M., Giannelli, M., Siciliano, G., Lazzarotti, G., Michelassi, M.C., Del Corona, A., Bartolozzi, C., Murri, L., 2005. Diffusion-tensor MR imaging of corticospinal tract in amyotrophic lateral sclerosis and progressive muscular atrophy. Radiology 237, 258–264. http://dx.doi.org/10.1148/radiol.2371041506.

Cosottini, M., Donatelli, G., Costagli, M., Caldarazzo Ienco, E., Frosini, D., Pesaresi, I., Biagi, L., Siciliano, G., Tosetti, M., 2016. High-resolution 7T MR imaging of the motor cortex in amyotrophic lateral sclerosis. AJNR Am. J. Neuroradiol. 37, 455–461. http://dx.doi.org/10.3174/ajnr.A4562.

Deistung, A., Schäfer, A., Schweser, F., Biedermann, U., Turner, R., Reichenbach, J.R., 2013a. Toward in vivo histology: a comparison of quantitative susceptibility mapping (QSM) with magnitude-, phase-, and R2*-imaging at ultra-high magnetic field strength. NeuroImage 65, 299–314. http://dx.doi.org/10.1016/j.neuroimage.2012.09.055.

Deistung, A., Schweser, F., Wiestler, B., Abello, M., Roethke, M., Sahm, F., Wick, W., Nagel, A.M., Heiland, S., Schlemmer, H.-P., Bendszus, M., Reichenbach, J.R., Radbruch, A., 2013b. Quantitative susceptibility mapping differentiates between blood depositions and calcifications in patients with glioblastoma. PLoS One 8, e57924. http://dx.doi.org/10.1371/journal.pone.0057924.

Denk, C., Rauscher, A., 2010. Susceptibility weighted imaging with multiple echoes. J. Magn. Reson. Imaging 31, 185–191. http://dx.doi.org/10.1002/jmri.21995.

Denk, C., Torres, E.H., MacKay, A., Rauscher, A., 2011. The influence of white matter fibre orientation on MR signal phase and decay. NMR Biomed. 24, 246–252. http://dx.doi.org/10.1002/nbm.1581.

Duyn, J.H., van Gelderen, P., Li, T.-Q., de Zwart, J.A., Koretsky, A.P., Fukunaga, M., 2007. High-field MRI of brain cortical substructure based on signal phase. Proc. Natl. Acad. Sci. U. S. A. 104, 11796–11801. http://dx.doi.org/10.1073/pnas.0610821104.

Haacke, E.M., Mittal, S., Wu, Z., Neelavalli, J., Cheng, Y.C.N., 2009. Susceptibility-weighted imaging: technical aspects and clinical applications, part 1. AJNR Am. J. Neuroradiol. 30, 19–30. http://dx.doi.org/10.3174/ajnr.A1400.

Haacke, E.M., Liu, S., Buch, S., Zheng, W., Wu, D., Ye, Y., 2015. Quantitative susceptibility mapping: current status and future directions. Magn. Reson. Imaging 33, 1–25. http://dx.doi.org/10.1016/j.mri.2014.09.004.

Hallgren, B., Sourander, P., 1958. The effect of age on the non-haemin iron in the human brain. J. Neurochem. 3, 41–51. http://dx.doi.org/10.1111/j.1471-4159.1958.tb12607.x.

Ignjatović, A., Stević, Z., Lavrnić, S., Daković, M., Bačić, G., 2013. Brain iron MRI: a biomarker for amyotrophic lateral sclerosis. J. Magn. Reson. Imaging 38, 1472–1479. http://dx.doi.org/10.1002/jmri.24121.

Ince, P.G., Evans, J., Knopp, M., Forster, G., Hamdalla, H.H.M., Wharton, S.B., Shaw, P.J., 2003. Corticospinal tract degeneration in the progressive muscular atrophy variant of ALS. Neurology 60, 1252–1258. http://dx.doi.org/10.1212/01.WNL.0000058901.75728.4E.

Knyazeva, M.G., 2013. Splenium of corpus callosum: patterns of interhemispheric interaction in children and adults. Neural Plast. 2013, 639430. http://dx.doi.org/10.1155/2013/639430 (12).

Kwan, J.Y., Jeong, S.Y., van Gelderen, P., Deng, H.-X., Quezado, M.M., Danielian, L.E., Butman, J.A., Chen, L., Bayat, E., Russell, J., Siddique, T., Duyn, J.H., Rouault, T.A., Floeter, M.K., 2012. Iron accumulation in deep cortical layers accounts for MRI signal abnormalities in ALS: correlating 7 tesla MRI and pathology. PLoS One 7, e35241. http://dx.doi.org/10.1371/journal.pone.0035241.

LeVine, S.M., Wulser, M.J., Lynch, S.G., 1998. Iron quantification in cerebrospinal fluid. Anal. Biochem. 265, 74–78. http://dx.doi.org/10.1006/abio.1998.2903.

Li, W., Wu, B., Liu, C., 2011. Quantitative susceptibility mapping of human brain reflects spatial variation in tissue composition. NeuroImage 55, 1645–1656. http://dx.doi.org/10.1016/j.neuroimage.2010.11.088.

Li, W., Wu, B., Batrachenko, A., Bancroft Wu, V., Morey, R.A., Shashi, V., Langkammer, C., Bellis, M.D., Ropele, S., Song, A.W., Liu, C., 2014. Differential developmental trajectories of magnetic susceptibility in human brain gray and white matter over the lifespan. Hum. Brain Mapp. 35, 2698–2713. http://dx.doi.org/10.1002/hbm.22360.

Lim, I.A.L., Faria, A.V., Li, X., Hsu, J.T.C., Airan, R.D., Mori, S., van Zijl, P.C.M., 2013. Human brain atlas for automated region of interest selection in quantitative susceptibility mapping: application to determine iron content in deep gray matter structures. NeuroImage 82, 449–469. http://dx.doi.org/10.1016/j.neuroimage.2013.05.127.

Liu, C., Li, W., Tong, K.A., Yeom, K.W., Kuzminski, S., 2015. Susceptibility-weighted imaging and quantitative susceptibility mapping in the brain. J. Magn. Reson. Imaging 42, 23–41. http://dx.doi.org/10.1002/jmri.24768.

Penfield, W., Rasmussen, T., 1950. The Cerebral Cortex of Man. Macmillan.

Philips, T., Robberecht, W., 2011. Neuroinflammation in amyotrophic lateral sclerosis: role of glial activation in motor neuron disease. The Lancet Neurology 10, 253–263. http://dx.doi.org/10.1016/S1474-4422(11)70015-1.

Putnam, M.C., Steven, M.S., Doron, K.W., Riggall, A.C., Gazzaniga, M.S., 2010. Cortical projection topography of the human splenium: hemispheric asymmetry and individual differences. J. Cogn. Neurosci. 22, 1662–1669. http://dx.doi.org/10.1162/jocn.2009.21290.

Schofield, M.A., Zhu, Y., 2003. Fast phase unwrapping algorithm for interferometric applications. Opt. Lett. 28, 1194–1196. http://dx.doi.org/10.1364/OL.28.001194.

Schweitzer, A.D., Liu, T., Gupta, A., Zheng, K., Seedial, S., Shtilbans, A., Shahbazi, M., Lange, D., Wang, Y., Tsiouris, A.J., 2015. Quantitative susceptibility mapping of the motor cortex in amyotrophic lateral sclerosis and primary lateral sclerosis. AJ. Am. J. Roentgenol. 204, 1086–1092. http://dx.doi.org/10.2214/AJR.14.13459.

Schweser, F., Deistung, A., Lehr, B.W., Reichenbach, J.R., 2010. Differentiation between diamagnetic and paramagnetic cerebral lesions based on magnetic susceptibility mapping. Med. Phys. 37, 5165–5178.

Schweser, F., Deistung, A., Lehr, B.W., Reichenbach, J.R., 2011. Quantitative imaging of intrinsic magnetic tissue properties using MRI signal phase: an approach to in vivo brain iron metabolism? NeuroImage 54, 2789–2807. http://dx.doi.org/10.1016/j.neuroimage.2010.10.070.

Strong, M., Rosenfeld, J., 2015. Amyotrophic lateral sclerosis: a review of current concepts. Amyotroph. Lateral Scler. Other Motor Neuron Disord. 4, 136–143. http://dx.doi.org/10.1080/14660820310011250.

Turner, M.R., Cagnin, A., Turkheimer, F.E., Miller, C.C.J., Shaw, C.E., Brooks, D.J., Leigh, P.N., Banati, R.B., 2004. Evidence of widespread cerebral microglial activation in amyotrophic lateral sclerosis: an [11C](*R*)-PK11195 positron emission tomography study. Neurobiol. Dis. 15, 601–609. http://dx.doi.org/10.1016/j.nbd.2003.12.012.

Wharton, S., Bowtell, R., 2015. Effects of white matter microstructure on phase and susceptibility maps. Magn. Reson. Med. 73, 1258–1269. http://dx.doi.org/10.1002/mrm.25189.

Wu, B., Li, W., Avram, A.V., Gho, S.-M., Liu, C., 2012. Fast and tissue-optimized mapping of magnetic susceptibility and T2* with multi-echo and multi-shot spirals. NeuroImage 59, 297–305. http://dx.doi.org/10.1016/j.neuroimage.2011.07.019.

Yousry, T.A., Schmid, U.D., Alkadhi, H., Schmidt, D., Peraud, A., Buettner, A., Winkler, P., 1997. Localization of the motor hand area to a knob on the precentral gyrus. A new landmark. Brain 120 (Pt 1), 141–157.